Smart Materials and Structures

A simulated annealing technique for multiobjective optimization of intelligent structures

To cite this article: A Chattopadhyay and C E Seeley 1994 *Smart Mater. Struct.* **3** 98

Smart Mater. Struct. 3 (1994) 98–106. Printed in the UK

A simulated annealing technique for multiobjective optimization of intelligent structures

Aditi Chattopadhyay and Charles E Seeley
Department of Mechanical and Aerospace Engineering, Arizona State University, Tempe, AZ 85287, USA

Received 6 October 1993, accepted for publication 4 February 1994

Abstract. A multiobjective optimization procedure is developed to address the combined problems of the synthesis of structures/controls and the actuator-location problem for the design of intelligent structures. Continuous and discrete variables are treated equally in the formulation. Multiple and conflicting design objectives such as vibration reduction, dissipated energy, power and a performance index are included by utilizing an efficient multiobjective optimization formulation. Piezoelectric materials are used as actuators in the control system. A simulated annealing algorithm is used for optimization and an approximation technique is used to reduce computational effort. A numerical example using a cantilever box beam demonstrates the utility of the optimization procedure when compared with a previous nonlinear programming technique.

1. Introduction

Aerospace structures must often compromise stiffness to meet stringent weight requirements. The reduced stiffness results in a vulnerability to resonance from relatively minor disturbance forces which would normally not present a problem. Therefore, it is important that these structures are able to suppress vibrations from an unknown disturbance force, using an active control system. Recently, there has been a significant interest in the design of intelligent structures for vibration control [1–3]. Several different areas are important to include in the design of an intelligent structure. First, the design of the structure must be considered [4]. This includes selection of a structural material and fabrication of structural members. Second, the design of the control system and actuators must be considered [3, 5]. Finally, the location of the sensors and actuators must be included in the design process as well [6, 7]. Previously these problems have been considered separately or sequentially. Since these areas are highly coupled, it is desirable to integrate design objectives from the different disciplines into a single optimization formulation to achieve a better intelligent structure than by considering these aspects sequentially.

Since several design objectives are used to address the areas of structures and controls, it is necessary to incorporate an efficient multiobjective optimization technique. The structures/controls problems are associated with continuous design variables such as thicknesses and gains. These variables exhibit derivatives and lend themselves well to gradient-based optimization techniques. The actuator-location problem involves discrete (0,1) variables which do not possess conventional derivatives. Therefore, combining these areas represents a formidable difficulty due to the incompatibility of continuous and discrete variables. Continuous variables can be represented by a series of discrete (0,1) variables which are then compatible with discrete optimization techniques such as simulated annealing. Simulated annealing algorithms have been shown to be effective in a variety of different engineering applications such as composites [8], actuator locations [6] and circuit board design [9]. In this paper, a procedure is developed to address a multiobjective optimization problem which includes both discrete and continuous design variables using simulated annealing. Since exact function evaluations are expensive, an approximation technique based on a linear Taylor series expansion is used to reduce computational effort. The procedure developed is then applied to a structures/controls optimization problem.

2. Problem formulation

In this study, aluminium box-beam elements are used for the structural components. A piezoceramic material (PZT G-1195) [10] with thickness 0.019 mm is used to model the actuators which are surface bonded to the box beam and act to provide a bending moment about the neutral axis of the beam elements from an applied voltage. Details of this model, using only continuous design variables and a nonlinear programming technique, have

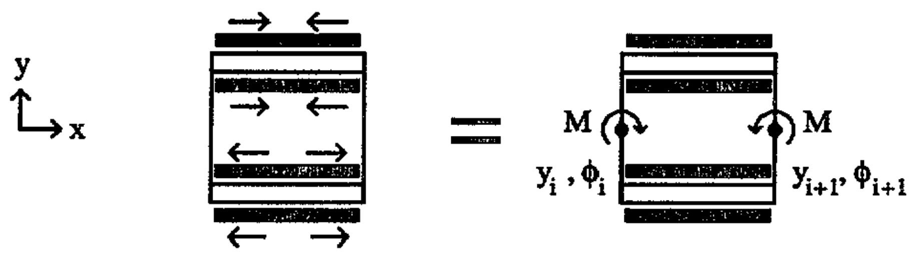

Figure 1. Active piezoelectric beam elements.

been previously developed using a finite-elements formulation [11]. The bending moment provided by the piezoelectric actuators is assumed to be equivalent to an applied moment M at the nodes of each beam element as shown in figure 1. This bending moment is the active control force used to control the structure. The dynamic equations of motion, without damping or disturbance force, assume the following standard form:

$$\mathbf{M}^*\ddot{x} + \mathbf{K}^*x = 0 \tag{1}$$

where x is the vector of transverse displacements and rotations $(y_1, \phi_1, y_2, \phi_2, \ldots)$, $\mathbf{M}^*$ is the augmented mass matrix and $\mathbf{K}^*$ is the augmented stiffness matrix which include mass and stiffness properties of the piezoelectrics only where they exist on the structure. A disturbance force F is applied to the uncontrolled structure over a time interval $0 \leqslant t \leqslant t_a$ which leads to the following equation of motion:

$$\mathbf{M}^*\ddot{x} + \mathbf{K}^*x = F. \tag{2}$$

The actuators become active during a time period $t_a \leqslant t \leqslant t_b$ in order to damp out the vibrations caused by the disturbance during the previous time period. The state space equations are written as:

$$\frac{\mathrm{d}}{\mathrm{d}t}\begin{bmatrix} x \\ \dot{x} \end{bmatrix} = \mathbf{A}\begin{bmatrix} x \\ \dot{x} \end{bmatrix} + \mathbf{B}[u] \tag{3}$$

where:

$$\mathbf{A} = \begin{bmatrix} \mathbf{0} & \mathbf{I} \\ -\mathbf{M}^{*-1}\mathbf{K}^* & \mathbf{0} \end{bmatrix} \tag{4}$$

$$\mathbf{B} = \begin{bmatrix} \mathbf{0} \\ -\mathbf{M}^{*-1}\mathbf{C} \end{bmatrix}. \tag{5}$$

It is assumed that the actuators and sensors are collocated in order to avoid problems with stability. In the above equations, $\mathbf{I}$ is the identity matrix and $\mathbf{C}$ is the gain matrix of the piezoelectric actuators. Rate feedback is used in conjunction with the control system so that the effect of the actuators will be similar to structural damping. The feedback control law is written as:

$$u = \mathbf{C}\dot{x}. \tag{6}$$

Therefore, the control gain matrix acts in an analogous manner to a viscous structural damping matrix and the actuators assume the role of active damper elements. Any passive structural damping is considered negligible. Finally, the undamped system is checked during the time interval $t_b \leqslant t \leqslant t_c$ to ensure that the total energy of the system and the displacements have been reduced to a specified value [3].

Modal summation techniques are used to reduce the equations of motion to a modal system. This transformation has considerable computational advantages and also eliminates problems related to controlling higher modes which do not have significant contributions on the overall motion. The first four bending modes are retained in this study. The active damping matrix, $\mathbf{C}$, is not proportional to the mass and stiffness matrices, so techniques which take advantage of that situation are not applicable here. As a result, the equations do not decouple.

3. Optimization formulation

3.1. Objective functions

The optimum design of intelligent structures is associated with several design criteria. The objective functions and constraints used in this study have been previously formulated [12] using continuous design variables and a nonlinear programming (NLP) technique. One of the objectives is to minimize the energy dissipated by the piezoelectric actuators. This has the effect of minimizing the work the actuators must do to control the structure. The energy dissipated by each actuator can be expressed as the integral over the time period of active control ($t_a \leqslant t \leqslant t_b$) for each actuator. The total energy to be minimized, J, is the sum of these integrals and is given as follows:

$$J = \sum_{i=1}^{\mathrm{IACT}} \int_{t_a}^{t_b} \dot{x}_i^{\mathrm{T}} \mathbf{c}_i \dot{x}_i \, \mathrm{d}t \tag{7}$$

where IACT is the current number of elements which contain actuators and $\mathbf{c}_i$ is the individual gain matrix of the ith active damping element. The total energy J can also be viewed as a quadratic performance index from a controls standpoint using the gain matrix as the arbitrary weight matrix which has real physical significance in this case.

Power requirements for piezoelectric control systems are an important issue in critical aerospace applications [13]. It is desirable to minimize the amount of electrical energy, U, required by the actuators to control the structure. Therefore it is used as an objective function. For the piezoelectric material used as an actuator, it is assumed that the applied electric field is much greater than the charge generated when the material is deformed. Piezoelectric actuators can be modeled as a parallel RC circuit where R_i is the resistivity and C_i is the capacitance of the ith piezoelectric actuator. The electrical energy U is an integral of power over time and is summed over all of the actuators for the total electrical energy which is expressed as follows:

$$U = \sum_{i=1}^{\mathrm{IACT}} \int_{t_a}^{t_b} \left\{ \frac{V_i^2}{R_i} + C_i V_i \frac{\mathrm{d}V_i}{\mathrm{d}t} \right\} \mathrm{d}t. \qquad (8)$$

In the above equation, V_i is the voltage of the ith actuator.

Vibration reduction is an important design criterion. Minimization of a performance index defined by the integral absolute error (IAE) criterion [14] is suitable for reducing overall vibrational amplitudes and is expressed as follows:

$$\int_{t_a}^{t_b} |\bar{e}(t)| \mathrm{d}t \qquad (9)$$

where $e(t)$ is the error in the system. Minimization of the IAE criterion results in a system with reasonable damping and a satisfactory transient-response characteristic. It is also easily evaluated numerically. Therefore the IAE criterion is used as an objective function which is minimized during optimization to reduce oscillatory motion. Since the desired input of the system approaches zero, the error can be represented simply as the state vector which contains both the displacements and velocities of the dynamic system:

$$e(t) = \begin{bmatrix} x \\ \dot{x} \end{bmatrix}. \qquad (10)$$

The integral is evaluated numerically over each component of the state vector and a 2-norm of the resultant vector is used to facilitate its usefulness in the optimization procedure. Finally, the fundamental frequency ω_1 is maximized to avoid possible resonance with the forcing frequency and thereby help reduce vibration.

3.2. Constraints

The design criteria that are formulated as constraints are discussed in this section. It is desired that the total energy E of the structure, which is the sum of the potential and the kinetic energies, is reduced to a specified fraction of the original energy after the time interval $T = t_b - t_a$. Therefore, a constraint is imposed as follows:

$$E_{\mathrm{fin}} \leqslant \gamma E_{\mathrm{int}} \qquad (11)$$

where E is the energy and the subscripts 'int' and 'fin' refer to the initial and the final states respectively. The quantity γ is the desired fraction of the initial energy remaining in the system after the specified time T.

A piezoelectric material is associated with a maximum electric field E_{max}. Exceeding this value can result in the loss of the material's special properties. Correspondingly, there exists a maximum voltage V_{max} that can be applied to a piezoelectric actuator and must not be exceeded. The voltage is checked at each time step of the numerical equation solver. Noting that $V_i = G_i \dot{\phi}_i$ for each actuator, when $V_i \geqslant V_{\mathrm{max}}$, saturation of the actuators occurs and the gain for the next time step for that actuator is set to:

$$G_i = \frac{V_{\mathrm{max}}}{\dot{\phi}_i}. \qquad (12)$$

This ensures that $V_i \leqslant V_{\mathrm{max}}$ without introducing any new design variables. As the rotational velocity increases, the voltage to each actuator remains constant and does not exceed the maximum allowable voltage. As the number of actuators is reduced during the optimization process, the voltage to the remaining actuators increases to redistribute the control forces necessary for satisfying all of the constraints. As a result, this constraint becomes more active.

The desired modal damping ratio $\bar{\zeta}_j$, corresponding to the jth mode, can be expressed as:

$$\bar{\zeta}_j = \frac{\ln(1/\kappa)}{\omega_j T} \qquad (13)$$

where ω_j is the jth undamped natural frequency of the structure and κ is the fraction of the initial vibration amplitude which remains after the time interval T. Upon calculation of ζ_j, the actual damping ratio corresponding to the jth mode, the following constraint is imposed to ensure that the desired damping ratios are achieved.

$$\zeta_j \geqslant \bar{\zeta}_j \qquad (14)$$

The gain matrix $\mathbf{C}$ is not constant since it must be altered at each time step to ensure that the voltage does not exceed V_{max}. Therefore ζ_j is not constant over time either. A minimum gain matrix is obtained at maximum velocity when saturation occurs. The maximum gain matrix is found when V_{max} is not exceeded by any one of the actuators. To evaluate the damping ratio constraint, constant damping ratios are determined using a gain matrix which is averaged over the time interval when the actuators are active. Although these averaged damping ratios cannot be used to construct an analytical solution of the decaying motion, they approximately describe the character of the solution to ensure that proper damping does occur in the desired modes. It is assumed that the disturbance force has a lower frequency than the natural frequency of the structure. By increasing the natural frequency of the structure, the interval between the natural frequency of the structure and the frequency of the disturbance force increases, which reduces the response of the structure to the disturbance force. Since the mass can increase in an effort to stiffen the structure and thereby minimize the energy dissipated by the actuators, a constraint is also imposed on the total mass of the beam and the actuators. The design variables include web thicknesses of each square box-beam element, gains of the actuators and actuator locations.

4. Optimization implementation

4.1. Optimization problem

The multiobjective optimization problem requires that both discrete (0,1) and continuous design variables be included in the formulation. Typical continuous design variables exhibiting at least first-order derivatives include parameters such as box-beam web thicknesses and gains. These variables are commonly used in gradient-based optimization procedures. The discrete (0,1) variables, which are easily adapted to represent the absence/presence of a sensor and actuator pair at a particular location on the structure, do not possess conventional derivatives. Therefore, these discrete variables are not compatible with conventional gradient-based optimization procedures and require discrete optimization techniques. Since the combined structures/controls and actuator-location problems include both continuous and discrete design variables, the combined optimization problem can be written as follows:

$$\begin{array}{lll} \text{Minimize} & F_K(\boldsymbol{a}_I, \boldsymbol{b}_J) & K = 1,2,\ldots,\text{NOBJ} \\ \text{Subject to} & g_M(\boldsymbol{a}_I, \boldsymbol{b}_J) & M = 1,2,\ldots,\text{NCON} \\ & & I = 1,2,\ldots,\text{NC} \\ & & J = 1,2,\ldots,\text{ND} \end{array}$$

$$\boldsymbol{a}_{\mathrm{L}} \leqslant \boldsymbol{a} \leqslant \boldsymbol{a}_{\mathrm{U}}$$

where NOBJ is the number of objective functions and NCON is the number of constraints. Additionally, $\boldsymbol{a}$ is the vector of continuous variables and $\boldsymbol{b}$ is the vector of (0,1) variables. The number of continuous design variables is NC and the number of discrete design variables is ND. Upper and lower bounds on the continuous variables are $\boldsymbol{a}_{\mathrm{L}}$ and $\boldsymbol{a}_{\mathrm{U}}$ respectively. The continuous design variables can be represented by a linear combination of discrete variables and selecting specific numerical values which the continuous variables can assume. For example, these values could correspond to standard values of pipe diameters or sheet thicknesses. The transformation from continuous variables to (0,1) variables is as follows [15]

$$a_I = z_{I1}d_{I1} + z_{I2}d_{I2} + \ldots + z_{IQ}d_{IQ}$$

with

$$z_{I1} + z_{I2} + \ldots + z_{IQ} = 1$$

and

$$z_{IQ} = 0 \text{ or } 1.$$

Thus, the Ith continuous design variables can take on the value of any of Q prescribed values d_{IQ}. The new design variable vector consists of the new discrete variables z_{IQ} used to represent the continuous variables in addition to the original discrete variables $\boldsymbol{b}_J$. Therefore, the objective functions and constraints can be totally represented by discrete (0,1) design variables and the new discrete optimization problem can partially be stated as follows:

$$\begin{array}{lll} \text{Minimize} & F_K(z_{IQ}, \boldsymbol{b}_J) & K = 1,2,\ldots,\text{NOBJ} \\ \text{Subject to} & g_M(z_{IQ}, \boldsymbol{b}_J) & M = 1,2,\ldots,\text{NCON}. \end{array}$$

An optimal solution cannot be guaranteed for a discrete optimization problem without evaluating every possible combination of (0,1) variables which is computationally impractical. Near optimal solutions can be obtained, however, with significant improvements in all objective functions with a reasonable amount of computational effort. Simulated annealing has the ability to climb out of local minima, unlike NLP techniques which often get 'stuck' in similar situations. It must be noted that, as with all discrete programming procedures, it is possible that not all constraints are satisfied exactly.

4.2. Approximate analysis

It is computationally expensive to compute exact function evaluations during each search of the design space. Therefore, an approximate technique, based on a linear Taylor series expansion, is used.

$$F_K^*(\boldsymbol{a}, \boldsymbol{b}) = F_K^*(\boldsymbol{a}_0, \boldsymbol{b}_0) + \sum_{I=1}^{\mathrm{NC}} \frac{\mathrm{d}F_K}{\mathrm{d}a_I}[a_I - a_{I_0}] + \sum_{J=1}^{\mathrm{ND}} \frac{\mathrm{d}F_K}{\mathrm{d}b_J}[b_J - b_{J_0}] \tag{15}$$

where $F_K^*(\boldsymbol{a}, \boldsymbol{b})$ is the linearized formulation of each objective function. The initial point for the approximation is $(\boldsymbol{a}_0, \boldsymbol{b}_0)$. Gradients of the continuous design variables can be computed by analytical means whenever possible, or by a finite-difference technique. 'Gradients' of the discrete variables $(\mathrm{d}F_K/\mathrm{d}b_J)$ which represent the sensitivity of the design to the absence/presence of an actuator are computed by calculating the quantity $\Delta F = F(1) - F(0)$ or $\Delta F = F(0) - F(1)$ for each actuator location, depending on whether or not an actuator is present at each location in the initial design. Similar expressions are used for the constraints.

During optimization, the approximate problem is solved and the solution is used as a seed point for the next linear approximation. The process is repeated until a satisfactory solution is found. Move limits are imposed on the continuous design variables to protect the validity of the approximation.

4.3. Multiobjective formulation

Simulated annealing must be applied to minimize a single, unconstrained objective function. Therefore, the Kreisselmeier–Steinhauser (KS) function approach is used to combine efficiently multiple and conflicting design objectives and constraints into a single unconstrained function which can be then minimized [16]. Recent studies have successfully demonstrated the usefulness of the KS function technique in multiobjective optimization problems [17]. In the KS formulation, each original objective function is transformed into a reduced objective function as follows:

$$\bar{F}_K = \frac{F_K^*}{F_{K_0}^*} - 1 - g_{\max} \leqslant 0 \qquad K = 1,2,\ldots,\text{NOBJ} \tag{16}$$

where $\bar{F}_K$ are the reduced objective functions, F_K^* are the original linearized objective functions, $F_{K_0}^*$ are their initial values and $g_{\max}$ is the maximum constraint.

Because these reduced objective functions are analogous to the previous constraints, a new constraint vector g_N is introduced where $N = \text{NCON} + \text{NOBJ}$. The new KS objective function to be minimized is then defined as

$$F = g_{N_{\max}} + \frac{1}{\rho} \ln \sum_{N=1}^{\text{NCON}+\text{NOBJ}} \exp\{\rho(g_N - g_{N_{\max}})\} \quad (17)$$

where the multiplier ρ is analogous to a draw-down factor controlling the distance from the surface of the KS function to the surface of the maximum function value.

4.4. Simulated annealing

Simulated annealing algorithms have been applied to a wide variety of engineering problems. Briefly, to minimize an objective function F, the algorithm can be stated as follows:

START
Current design is F
Perturb current design F_{new}
If $F_{new} \leqslant F$ *then*
  $F = F_{new}$
Else if $P_{acc} \leqslant P$ *then*
  $F = F_{new}$
End if
Go to START

The acceptance probability P_{acc} of retaining a worse design is computed as follows:

$$P_{acc} = \exp(-1/T) \quad (18)$$

where T is the 'temperature' which is reduced for successive iterations, thus reducing the probability of accepting a worse design, and P is a random number such that $0 \leqslant P \leqslant 1$. Occasionally accepting a worse design under the given probability allows the algorithm to climb out of possible local minima. The above loop is repeated a set number of times for each approximate analysis. The minimized design is then used as a seed point for the new approximation. This process is repeated until convergence is obtained as shown in figure 2.

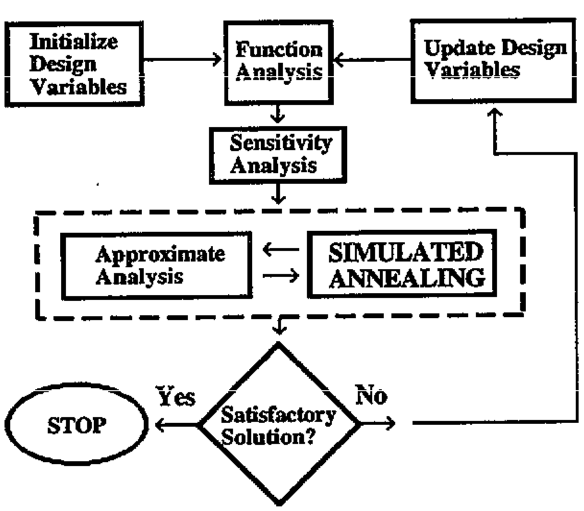

Figure 2. Flowchart of optimization procedure.

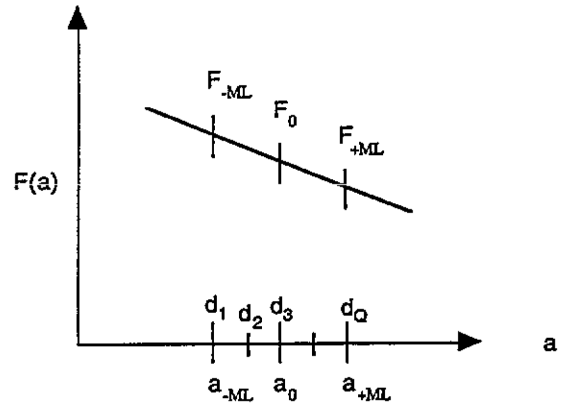

Figure 3. Discretization of move-limit interval.

4.5. Optimization procedure

Preselected values for the continuous variables, d_Q, can be determined in one of two ways. First, these values can be selected over the entire expected range of the variables corresponding to either standard values or evenly spaced intervals. The second method, which is used for the current study, involves discretizing the interval formed by the imposition of the move limits which are used to protect the validity of the approximation about the seed point $\boldsymbol{a}_0$. These methods apply to all continuous design variables, so the subscript I has been dropped for clarity. This interval can be divided up into any number of evenly spaced intervals as shown in figure 3. The subscripts $-$ML and $+$ML indicate the lower and upper bounds formed by the move limit. The expansion point for the Taylor series approximation is $\boldsymbol{a}_0$ and the constants d_Q represent Q possible values for $\boldsymbol{a}$. The continuous variables can be more accurately represented by increasing the number of points taken inside the interval, or by reducing the move limit interval. These values are determined at each iteration and must be altered as the seed point for each new approximation is relocated. This method also increases the efficiency of the simulated annealing algorithm compared to preselecting values of d_Q over the entire range of $\boldsymbol{a}$ since only those values for the design variables which satisfy the move limits can be selected. This eliminates the need for checking the design variables selected by the simulated annealing algorithm to ensure that the imposed move limits are not exceeded.

Exact function evaluations are the most computationally expensive aspect of the problem and the use of the approximate analysis significantly reduces the number of such exact function evaluations necessary. The actual simulated annealing algorithm with the approximate analysis is computationally inexpensive and takes a smaller percentage of the total computational effort than the exact objective function evaluations required to assemble the approximate analysis. Since the computational effort for the simulated annealing algorithm is

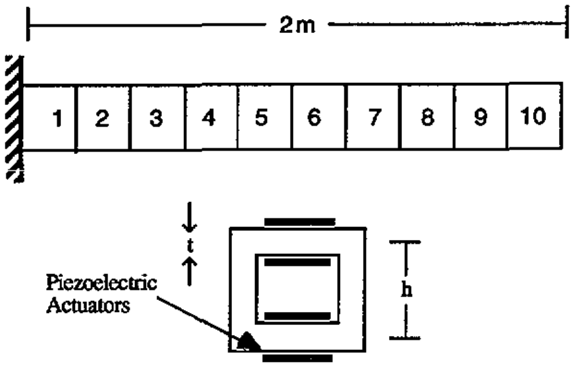

Figure 4. Cantilever box beam.

minimal, there is no reason to be conservative with the number of loops of the simulated annealing. The utility of the algorithm is demonstrated in the results, which show improved designs in all cases. The simulated annealing results are compared with those previously obtained using a nonlinear programming approach.

5. Results and discussion

The procedure developed is demonstrated through a numerical example of a cantilever box beam (figure 4). The beam is subjected to a sinusoidal disturbance force of 220 N applied to the tip of the box beam over a period of 0.067 s at a frequency of 25 Hz. Results are presented with the four objective functions previously described. These include the dissipated energy J, the electrical power U and an index of performance IAE which are all minimized. The natural frequency ω_1 is maximized by minimizing its negative value. Constraints are placed on the energy, applied voltage to the actuators, displacements and mass. Damping factor constraints are set such that the initial vibrational amplitudes of the first four modes are reduced to 5% of their original values after one second of active controls. The energy in the system, which is the sum of the potential and kinetic energies, must also be reduced to 5% of its initial value. For the mass constraint, a value of $\bar{m} = 3.5$ kg is used which is the maximum allowable mass of the beam and actuators. Design variables include box-beam web thicknesses, t_i, actuator locations, α_i and actuator gains. The gain of all of the actuators is set to be equal to reduce the dimension of the design variable vector. Upper and lower bounds are placed on the ith box-beam thickness such that $0.5\,\text{mm} \leqslant t_i \leqslant 2.5\,\text{mm}$. The height ($h$) of the beam is not altered during optimization and is set to 10 cm. The gain is constrained to be positive for stability. The absence or presence of the ith actuator is indicated by $\alpha_i = 0$ or $\alpha_i = 1$ respectively. An initial design is chosen where the web thickness for each box-beam element, t_i, is set to 1.5 mm as shown in table 1. The initial design violates both the mass constraint and the damping constraint corresponding to the first mode.

For the simulated annealing algorithm, the interval formed by the move limits is divided into 50 evenly spaced points ($Q = 50$). Each value of d_Q comprises one of these points for all of the continuous design variables that can be selected by the simulated annealing algorithm. Once the continuous variables are transformed into discrete variables, a total of 510 discrete variables are used during optimization. A random actuator configuration is chosen with actuators located on elements 1, 3, 5, 6, 7, 8 and 10. For this problem, 2000 loops of the simulated annealing algorithm are used for each optimization iteration. It must be noted that these loops are computationally inexpensive due to the implementation of the approximate analysis. Since there are 3.54×10^{23} possible combinations of the discrete variables, 2000 loops represents an extremely small portion of the actual design space. The value of the parameter ρ in the KS function is recommended to be in the range $5 \leqslant \rho \leqslant 200$ when used in conjunction with a nonlinear programming technique [18]. When used in the simulated annealing algorithm, a small value of $\rho = 10$ is found to be most appropriate. Larger values of ρ result in numerical instabilities due to jumps in the objective functions and/or constraints due to the use of discrete design variables. Move limits of 10% are placed on each design variable to protect the validity of the approximation. After 10 optimization iterations, ρ is increased to 20 and the move limits are reduced to 5%. A larger value of ρ moves the KS function envelope as close to the maximum violated constraint as possible while a smaller

Table 1. Optimization results: simulated annealing and NLP.

	Simulated annealing				NLP			
Element	Initial t_i (mm)	α_i	Final t_i (mm)	α_i	Initial t_i (mm)	α_i	Final t_i (mm)	α_i
1	1.5	1	2.5	1	1.5	1	1.2	1
2	1.5	0	1.7	1	1.5	1	1.7	0
3	1.5	1	1.2	1	1.5	1	2.0	0
4	1.5	0	1.0	0	1.5	1	2.4	0
5	1.5	1	0.7	1	1.5	1	1.7	0
6	1.5	1	0.6	0	1.5	1	1.0	0
7	1.5	1	0.6	0	1.5	1	0.8	0
8	1.5	1	0.9	0	1.5	1	0.7	0
9	1.5	0	0.8	1	1.5	1	0.7	0
10	1.5	1	0.8	0	1.5	1	0.7	0

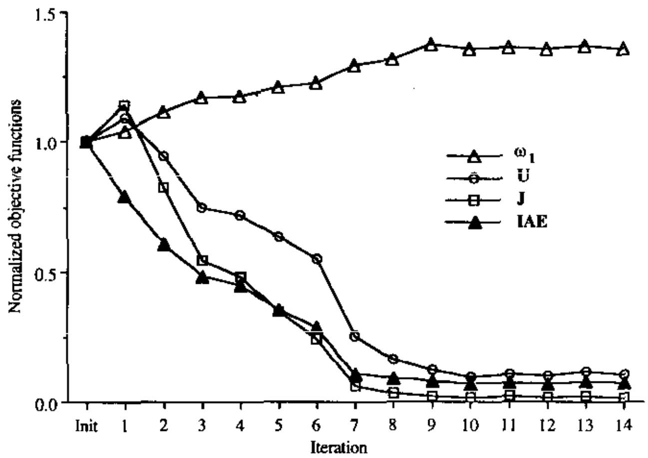

Figure 5. Objective function iteration history.

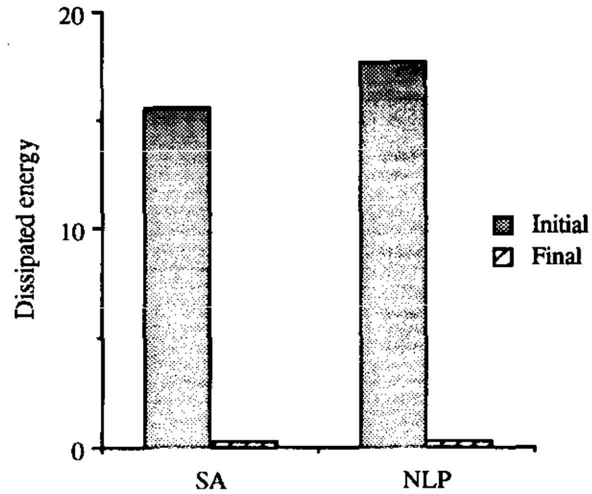

Figure 6. Comparison of dissipated energy.

value of ρ retains contributions of all of the objective functions and constraints. The reduced move limit allows smooth convergence of the optimization and a better approximation of the continuous design variables.

The optimum simulated annealing results are obtained after 14 iterations as shown in figure 5 where each original objective function is normalized to its initial value. This takes about 47 min of CPU time on an IBM RS6000 workstation. The final design consists of actuators at elements 1, 2, 3, 5 and 9 as shown in table 1. Improvements are made in all of the objective functions. The simulated annealing algorithm results in the dissipated energy, J, being reduced by 98% from the initial to the final design. The index of performance IAE and the electrical power consumption U are reduced by 93% and 89% respectively. The natural frequency, ω_1, which is maximized in the optimization formulation, increases by 36%. The damping ratio constraint on the first mode and the voltage constraint represent the most active constraints. The use of different initial actuator configurations also resulted in similar improvements to the objective functions.

The results obtained using the simulated annealing algorithm are compared with those obtained using continuous design variables based on an NLP technique where non-optimal actuators were eliminated on the basis of dissipated energy [12]. To describe the algorithm briefly, actuators were initially located at each possible location on the discretized structure which were elements of the finite-element discretization of the box beam. A single optimization iteration consisted of minimizing the objective functions using the current actuator configuration until either convergence or a maximum number of cycles (20) was reached. The actuator which dissipated the least amount of energy, compared with the remaining set of actuators, was eliminated as a possible actuator location. The new configuration was then re-optimized in the next iteration and another actuator was eliminated. The procedure was repeated until no more actuators could be eliminated from the set of possible actuator locations without violating one or more constraints. The nonlinear programming technique CONMIN [19] was used in conjunction with the KS function approach and a Taylor-series-based approximation was also used to reduce computational effort. The same initial design is used for both the NLP technique and the simulated annealing results except that actuators are initially located on each element for the NLP technique and a random actuator configuration is used for the simulated annealing. Tables 1 and 2 and figures 5–8 present results of the two optimization approaches.

Table 2. Additional optimization results.

	Simulated annealing		NLP	
	Initial	Final	Initial	Final
Dissipated energy (J)	15.58	0.25	17.65	0.31
Natural frequency (Hz)	29.73	40.47	30.62	39.81
IAE ($\times 10$)	86.56	6.27	65.04	5.78
Power (J)	6.93	0.74	8.09	0.76
Mass (kg)	4.18	2.96	4.54	3.01

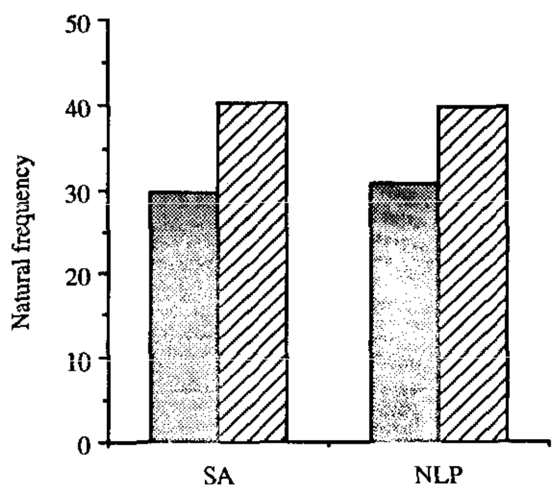

Figure 7. Comparison of natural frequency.

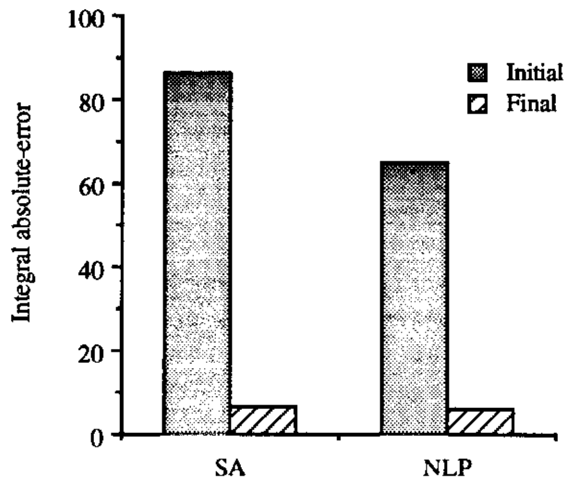

Figure 8. Comparison of IAE index.

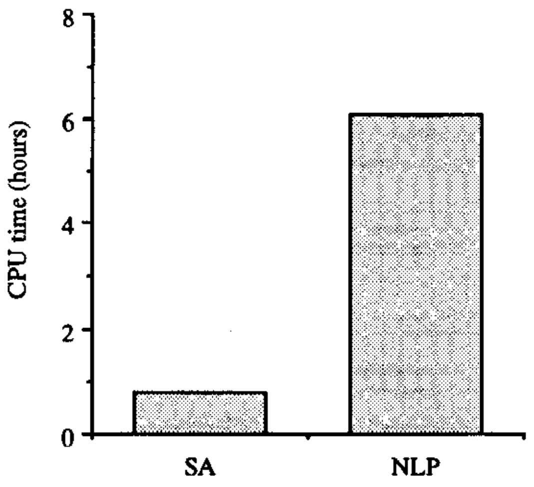

Figure 10. Comparison of CPU time.

The optimal configurations obtained using the two techniques differed significantly. From table 1 it is shown that the optimal configuration obtained using the NLP technique consists of a single actuator at element 1 in contrast to the optimal configuration obtained using the simulated annealing algorithm which comprises five actuators at elements 1, 2, 3, 5 and 9. In general, actuators at the tip of the beam are eliminated first for the NLP technique since they are less effective than those at the root of the box beam. Although the mass constraint is violated in the initial design in both cases, it is not active in the final design in either case. It must be noted that the mass of the optimized beam is slightly higher in the design obtained using simulated annealing due to the greater number of actuators than in the NLP final design. The thickness distribution obtained using the simulated annealing technique is consistent with expected trends. The beam is thickest at the root, and tapered towards the tip except for the last two elements where thickness increases. This is a result of the optimization effort to increase the stiffness of the beam at the location where the disturbance force is applied. The thickness distribution obtained using the NLP technique is more non-linear. This is possibly due to an effort to increase stiffness since a reduced number of actuators are present in the final design of this case. The four original objective functions for each approach are presented in figures 5–8 with original and final results for both the simulated annealing and the NLP techniques. It must be noted that the optimization results depend on the disturbance force used and may change for a different disturbance force. Improvements of the same order are made in all of the original objective functions using both techniques although final actuator configurations are different. This indicates the presence of possible local minima. The major difference is the amount of computational effort required in each case. The simulated annealing algorithm requires about one hour of CPU time whereas the NLP technique requires six hours of CPU time on the same platform to achieve optimum results as shown in figure 10. A total of 330 exact function evaluations are required for the simulated annealing while 220 evaluations are necessary for the NLP technique using CONMIN. The dramatic reduction in required CPU time for the simulated annealing algorithm indicates a significant improvement in efficiency compared to the NLP technique.

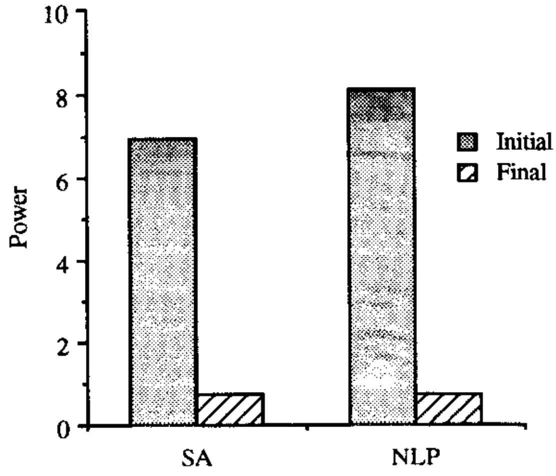

Figure 9. Comparison of power.

6. Concluding remarks

A multiobjective optimization procedure has been developed based on a simulated annealing technique to include both discrete and continuous design variables. The Kreisselmeier–Steinhauser multiobjective optimization approach was implemented to formulate the multiobjective optimization problem. An approximate analysis technique was used, based on a linear Taylor series expansion, to reduce the computational effort associated with exact function evaluations. A numerical example of a cantilever beam subjected to a sinusoidal disturbance force was presented. Objective functions included energy dissipation, power consumption, an index of performance for vibration control and natural frequency. Constraints were placed on total energy, voltage, displacements and mass. Design variables included actuator gains, box-beam web thicknesses and actuator locations. Significant improvements were obtained in all objective functions and optimal actuator locations were determined inside a closed-loop procedure. The results using this technique were compared with a previously used technique based on a nonlinear programming procedure. The following observations can be made from this study.

(1) Both continuous and discrete (0,1) design variables were included in the closed loop optimization procedure.
(2) The optimization procedure developed resulted in significant improvements in all objective functions while satisfying the imposed constraints.
(3) The procedure using simulated annealing resulted in substantial reductions in CPU time compared to the NLP technique.

References

[1] Hanagud S, Obal M W and Claise A J 1992 Optimal vibration control by the use of piezoceramic sensors and actuators *J. Guid. Control Dynam.* **15** 1199–205
[2] Miller D F and Shim J 1987 Gradient-based combined structural and control optimization *J. Guid.* **10** 291–8
[3] Horner G and Walz J 1985 A design methodology for determining actuator gains in spacecraft vibration control *Proc. 26th AIAA/ASME/ASCE/AHS/ASC Structures, Structural Dynamics and Materials Conf. (Orlando, FL, April 15–17, 1985)* (Washington, DC: AIAA) pp 143–51
[4] Sepulveda A E., Jin I M and Schmit L A Jr 1992 Optimal placement of active elements in control augmented structural synthesis *Proc. 33rd AIAA/ASME/ASCE/AHS/ASC Structures, Structural Dynamics and Materials Conf. (Dallas, TX, April 13–15, 1992)* (Washington, DC: AIAA) pp 2768–81
[5] Crawley E F and de Luis J 1987 Use of piezoelectric actuators as elements of intelligent structures *AIAA J.* **25** 1373–85
[6] Onoda J and Hanawa Y 1992 Optimal locations of actuators for statistical static shape control of large space structures: a comparison of approaches *Proc. 33rd AIAA/ASME/ASCE/AHS/ASC Structures, Structural Dynamics and Materials Conf. (Dallas, TX, April 13–15, 1992)* (Washington, DC: AIAA) pp 2788–95
[7] Zimmerman D C 1991 A Darwinian approach to the actuator number and placement problem with nonnegligible actuator mass *Proc. 13th Biennial Conf. on Mechanical Vibration and Noise, ASME Design Technical Conferences, DE Vol. 34, (Miami, FL, 1991)* pp 83–8
[8] Lombardi M, Haftka R T and Cinquini C 1992 Optimization of composite plates for buckling by simulated annealing *Proc. AIAA/ASME/ASCE/AHS/ASC Structures, Structural Dynamics and Materials Conf. (Dallas, TX, April 13–15, 1992)* (Washington, DC: AIAA) pp 2552–62
[9] Kirkpatrick S, Gelatt C D Jr and Vecchi M P 1983 Optimization by simulated annealing *Science* **220** 671–80
[10] 1993 *Piezo Systems Inc. Product Catalog*
[11] Seeley C E and Chattopadhyay A 1993 The development of an optimization procedure for the design of intelligent structures *Smart Mater. Struct.* **2** 135–46
[12] Seeley C E and Chattopadhyay A 1994 A multiobjective design optimization procedure for control of structures using piezoelectric materials *J. Intell. Mater. Syst. Struct.* at press
[13] Rogers C A 1993 Smart structures: where does the energy go? *Invited Technical Talk, SPIE North American Conf. on Smart Structures and Materials (Albuquerque, NM, February 1–4, 1993)* (Bellingham, WA: SPIE)
[14] Ogata K 1990 *Modern Control Engineering* (Englewood Cliffs, NJ: Prentice-Hall)
[15] Olsen G R and Vanderplaats G N 1989 Method for nonlinear optimization with discrete design variables *AIAA J.* **27** 1584–9
[16] Kreisselmeier G and Steinhauser R 1979 Systematic control design by optimizing a vector performance index *Int. Federation of Active Controls Symp. on Computer-Aided Design of Control Systems (Zurich, August 29–31, 1979)* pp 113–7
[17] Chattopadhyay A and McCarthy T 1991 Multiobjective design optimization of helicopter rotor blades with multidisciplinary couplings *Structural Systems and Industrial Applications* ed S Hernandez and C A Brebbia pp 451–61
[18] Wrenn G 1989 An indirect method for numerical optimization using the Kreisselmeier–Steinhauser function *NASA Contract Report 4220*
[19] Vanderplaats G N 1973 *CONMIN—A FORTRAN Program for Constrained Function Minimization User's Manual* (NASA) TMX-62,282